

Effect of finite crack length and blunting on dislocation nucleation in mode III

G. E. BELTZ and L. L. FISCHER

Department of Mechanical and Environmental Engineering, University of California, Santa Barbara, California 93106-5070, USA

[Received 7 May 1998 and accepted in revised form 4 August 1998]

ABSTRACT

Continuum models, based upon both the Volterra and the Peierls descriptions of a screw dislocation ahead of a mode III crack, are used to evaluate the critical loading for dislocation nucleation at the tip of a finite pre-blunted crack. Results are presented for various crack tip root radii, for several crack lengths. Moreover, the effect of ledge formation at the crack tip is evaluated. It is found that blunt cracks require a substantially larger load to induce dislocation nucleation, and this effect is amplified by including ledge formation in the analysis. It is also noted that short cracks require a reduced load for dislocation nucleation.

§1. INTRODUCTION

Understanding crack tip behaviour and the ductile-to-brittle transition has been the motivation behind a wide range of continuum and atomistic studies. One ongoing objective of this research is to understand whether a crack will respond to loading by emitting dislocations, or by propagating. The Rice–Thomson (1974) model was an early attempt to quantify the competition between dislocation emission and atomic decohesion using continuum concepts. In it, the competition between cleavage decohesion and dislocation emission is evaluated in terms of the parameters G_{cleave} , the ‘applied’ energy release rate associated with cleavage, and G_{disl} , the energy release rate associated with the emission of a single dislocation on a slip plane emanating from the crack tip. If $G_{\text{cleave}} < G_{\text{disl}}$, the crack propagates in a brittle manner; conversely, if $G_{\text{disl}} < G_{\text{cleave}}$, a dislocation moves away from the crack tip, thus blunting and ‘shielding’ the crack tip from further increases in applied loading (figure 1). Over the years, this framework has been broadened to account for elastic anisotropy, bimaterial interfaces, nonlinear core structures, realistic slip systems and three-dimensional dislocation geometries. Reviews of these efforts may be found in recent articles by Xu *et al.* (1995) and Rice *et al.* (1992).

Most mechanistic studies of dislocation formation have assumed that crack tips are atomically sharp prior to dislocation nucleation and remain so during the nucleation event. Kinematically, this is not the case, as incipient dislocation activity (at least when the slip plane is aligned with the crack plane) forces the crack faces to separate. More compelling support for this idea comes from atomistic studies of dislocation nucleation, which clearly show blunting at the atomic scale. Realistic crack tip geometries have received recent attention in the work of Schiøtz *et al.* (1996, 1997), in which a blunt crack tip was conformally mapped to the upper half of the complex plane. The mode III stress fields were derived using antiplane elasticity. Fischer and Beltz (1997) created a finite-element model to determine the

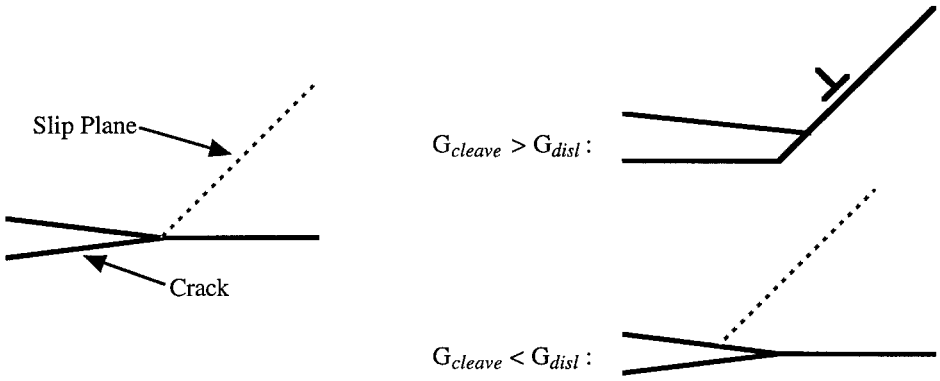


Figure 1. A sharp crack with intersecting slip plane (left), showing the competition between dislocation emission (upper right) and cleavage decohesion (lower right).

stress fields of a similar blunt crack tip under mode I loading. In both cases, the stress fields of blunted cracks were shown to deviate moderately from those of sharp cracks, especially at length scales of interest away from the tip. This deviation in stress field around the crack tip from the ideally sharp limit could very easily change the favourability of crack advancement versus dislocation emission. Neither of the above studies, however, yielded a critical load for dislocation nucleation.

Blunt crack geometries have also received limited attention in atomistic studies. Schiøtz *et al.* (1996, 1997) conducted simulations using a two-dimensional hexagonal atomistic model under mode I and mode II loading. They found that, for a blunting height of ten layers of atoms, the force required to propagate the crack was 15–20% more than that for a sharp crack. Gumbsch (1995) similarly found that crack tip geometry, particularly an increased blunting height, can significantly increase the required loading for crack propagation. Two-dimensional molecular dynamic simulations done by Paskin *et al.* (1985) also used a hexagonal lattice structure to observe the sensitivity of stress distribution to crack geometry. While the results showed little difference in the stress distributions for narrow and wide cracks, it was shown that irregularly shaped crack tips displayed significantly lower stresses in the near-tip region.

On the basis of the above, we hypothesize that deviations in crack tip geometry can change the favourability of crack advancement versus dislocation nucleation (both of which, presumably, are made more difficult by blunting, but not necessarily equally). Consideration of this effect should substantially contribute to the reconciliation between continuum-based and atomistic models. The purpose of the current paper is to provide a simple model, based upon screw dislocation emission from a pre-blunted shear crack loaded in mode III. This paper examines the effects of crack tip root radius (a measure of bluntness) and crack length on the critical mode III loading for dislocation nucleation at the tip of an elliptically shaped crack. The ellipse is used for analytical convenience and will allow us to draw some conclusions about crack size effects as well. An obvious trade-off here is that the elliptical crack tip profile does not retain the corner (and its associated stress singularity) that would result, at least from a continuum viewpoint, when dislocations emit along a single slip plane (figure 1). Immediately, this suggests that our elliptical representation will lead to an overestimate of the effects of blunting. Moreover, the geometry under

consideration is artificial in that the antiplane deformation associated with prior screw dislocation activity would *not* blunt a crack. Work in progress by Fischer and Beltz (1998) confirms that more applicable in-plane models (i.e. for dislocations with edge components in bodies loaded under Mode I) give identical trends, as well as the fact that conditions for cleavage also become less favourable as the crack blunts.

Two models will be presented in this paper. The first is based on continuum elastic dislocation theory and is analogous to the analytic model presented by Rice and Thomson (1974) and updated by Mason (1979) and Rice *et al.* (1990). The second model is based upon the Peierls framework (Rice 1992) to allow for extended nonlinear (but planar) dislocation cores. Both models use a thin elliptical hole as an initial unstressed reference state, that is, it is assumed that any dislocations which gave rise to the initial blunted configuration have moved infinitely far away, and small-strain elastic dislocation theory is subsequently used. The effect of additional stress sources (e.g. the back stresses due to dislocations present nearby the crack), as well as the full implications of using a small-strain analysis, are deferred to future work.

§2. DISLOCATION NUCLEATION IN THE VOLTERRA FRAMEWORK

The load for dislocation nucleation, expressible as G_{disl} (the energy release rate associated with nucleation), is derived in this section. The force tending to drive a straight pre-existing screw dislocation *away* from an elliptical cut-out (figure 2)

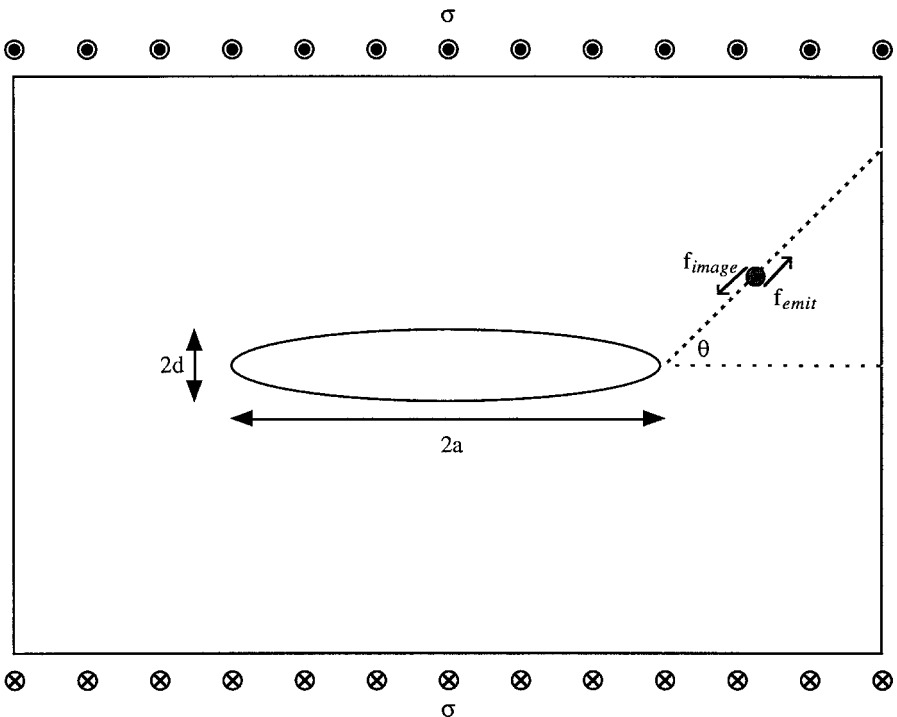


Figure 2. A screw dislocation in proximity to an elliptical crack under mode III loading experiencing the opposing Peach–Koehler and image forces.

is given by the Peach–Koehler formula, where σ_{ij} is taken as the stress field in an infinite plate containing an elliptical hole, loaded in antiplane shear (i.e. $\sigma_{yz} \rightarrow \sigma$ as $z \rightarrow \infty$) *without* the dislocation present, evaluated at the dislocation position:

$$f_{\text{emit}} = | - \varepsilon_{ijk} s_i \sigma_{jl} b_l \hat{\mathbf{e}}_k | = b \sigma_{\theta z} = b \operatorname{Re} \left(\frac{\sigma (g t^2 + 1)}{g (t^2 - 1)} \exp(i\theta) \right), \quad (1)$$

where ε_{ijk} is the permutation tensor, s_i is a unit vector describing the dislocation line direction, b_l is the Burgers vector (here taken parallel to the dislocation line), θ is the slip plane inclination angle, $g = (a - d)/(a + d)$, and $i = (-1)^{1/2}$. The Einstein index convention is assumed. The stress field is obtained via the conformal mapping

$$z = \frac{c}{2} \left(t + \frac{1}{t} \right), \quad (2)$$

where $c = (a^2 - d^2)^{1/2}$, which maps the ellipse of semiaxes a and d into a circle of radius $(1/g)^{1/2}$. An effective, or ‘apparent’, mode III stress intensity factor is defined as $\sigma(\pi a)^{1/2}$. We couch the problem in terms of K_{III} , bearing in mind that we are using a slender ellipse ($a \gg d$) to simulate a slit that macroscopically resembles a crack with a crack root radius $\rho = d^2/a$ that is of atomic dimension. Within the framework of linear elastic fracture mechanics, K_{III} remains a valid descriptor of the intensity of the stress field for distances away from crack tip that are small compared with a , but large compared with ρ .

The ‘image’ force component opposes outward motion of the dislocation line and draws it back into the tip. The image force for a screw dislocation arbitrarily located external to an elliptical hole was solved for by Zhang and Li (1991). They correctly recognized that the solution has two principal results, depending on whether the dislocation is introduced from the elliptical boundary ($m = 1$), or from the far field ($m = 0$). Their result is

$$f_{\text{image}} = \frac{\mu b^2}{2\pi} \operatorname{Re} \left[\frac{\exp(i\theta)}{(z_d^2 - c^2)^{1/2}} \left(\frac{-c}{2t_d(z_d^2 - c^2)^{1/2}} + \frac{1}{1 - g t_d \bar{t}_d} - m \right) \right], \quad (3)$$

where z_d denotes the position of the dislocation, μ is the shear modulus and t_d is the transformation of z_d according to equation (2). In our current application, the appropriate value for m is taken to be unity.

To find the critical stress intensity factor at which dislocation emission occurs, we use a simplified statement of the Rice–Thomson model that imposes $f_{\text{emit}} + f_{\text{image}} = 0$ for $r = r_c$, the dislocation core size, which also assures that $f_{\text{emit}} > f_{\text{image}}$ for all $r > r_c$. By combining equations (1) and (3) we can solve for the critical mode III stress intensity factor for screw dislocation emission at the elliptical crack tip. The critical mode III stress intensity factor can be converted into a critical energy release rate by invoking the Irwin-type energy release rate expression for mode III,

$$G = K_{III}^2 / 2\mu, \text{ yielding}$$

$$\bar{G} = \frac{G}{\gamma_{us}} = \frac{\pi^2 \bar{h} K_{III}^2}{\mu^2 b} = \frac{\frac{g^2 \pi \bar{h} a b}{4} \left(\text{Re} \left[\frac{\exp(i\theta)}{(z_d^2 - c^2)^{1/2}} \left\{ \frac{-c}{2t_d(z_d^2 - c^2)^{1/2}} + \frac{1}{1 - gt_d \bar{t}_d} - 1 \right\} \right] \right)^2}{\left(\text{Re} \left[\frac{\exp(i\theta)(gt_d^2 + 1)}{t_d^2 - 1} \right] \right)^2} \quad (4)$$

where $z_d = a + r_c \exp(i\theta)$.

As an example, figure 3 shows critical energy release rates for dislocation emission for various values of crack length and crack tip root radius when the slip plane is taken as the prolongation of the crack plane, that is $\theta = 0$. The energy release rates are normalized by the unstable stacking energy as given by the Frenkel (1926) model ($\gamma_{us} = \mu b^2 / 2\pi^2 h$), where the value of h/b or h is taken as $2^{1/2}$, appropriate for a Shockley partial dislocation in a fcc crystal. This particular normalization is chosen to facilitate comparisons in the next section, which explicitly makes use of the unstable stacking concept. The crack lengths and crack tip root radii are normalized by b . Equation (4) is similarly evaluated for $\theta = 60^\circ$ and specific results for this case are shown in figure 4.

**Critical Energy Release Rate of Nucleation
Volterra Framework
 $\theta = 0^\circ$**

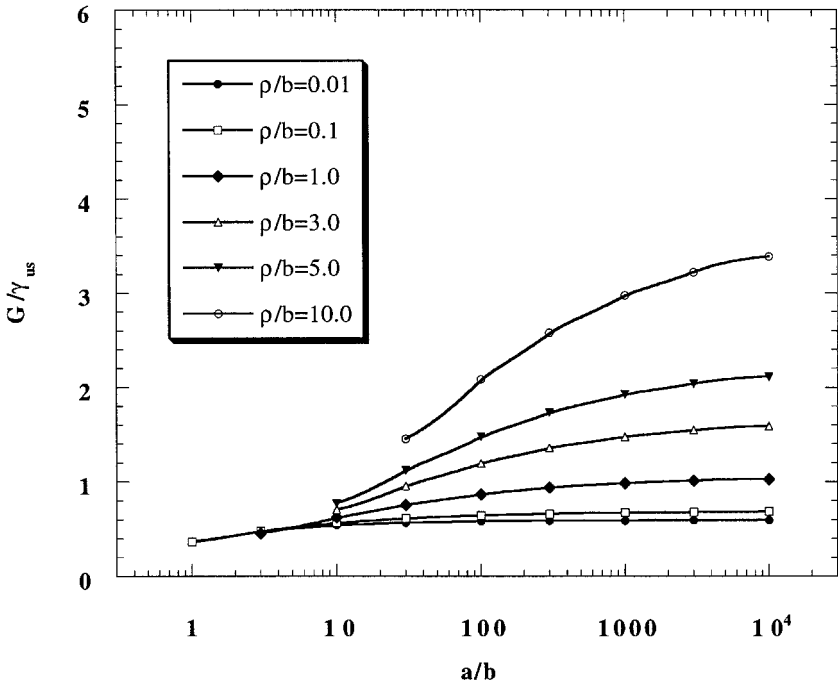


Figure 3. The critical energy release rates of screw dislocation nucleation for a slip plane inclination of 0° under mode III loading in the Volterra framework. Results are shown for various crack lengths and crack tip root radii.

Critical Energy Release Rate of Nucleation Volterra Framework

$$\theta = 60^\circ$$

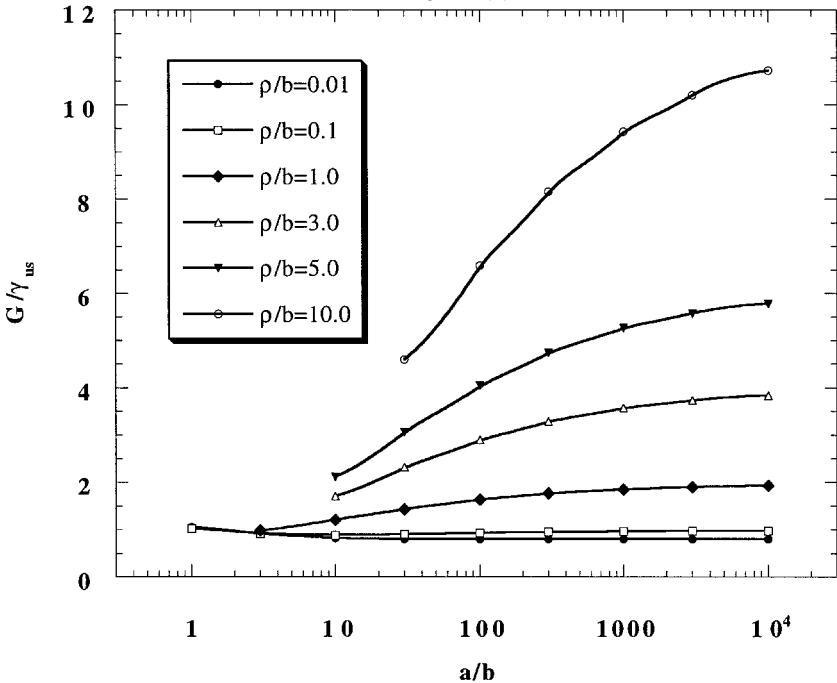


Figure 4. The critical energy release rates of screw dislocation nucleation for a slip plane inclination of 60° under mode III loading in the Volterra framework. Results are shown for various crack lengths and crack tip root radii.

Figures 3 and 4 reveal two principal behaviours. First, as expected, increasing the value of the crack tip root radius ρ increases the critical threshold for dislocation nucleation. The effect is rather pronounced. For example, for a relatively long crack, if the tip is assumed to have a root radius of just one atomic spacing (rather than being mathematically sharp), the critical energy release rate nearly doubles. For a root radius of just ten atomic spacings, the critical energy release rate is an order of magnitude larger. The crack tip root radii considered here are not large, even in an atomic sense and could easily be achieved by prior dislocation nucleation, diffusive or other relaxation processes; in fact, it is more realistic that a stationary crack takes on some degree of bluntness rather than remaining atomically sharp.

The second major conclusion to be drawn from this analysis is that, as the crack length decreases, so does the critical energy release rate. This effect is not observable for sharp cracks and manifests itself only when the root radius exceeds about one atomic spacing. For typical root radii considered here, it is necessary for a finite crack to exceed 10^2 – 10^4 Burgers vectors before the 'long-crack' limit is reproduced.

§3. THE PEIERLS MODEL AND RESULTS

The Peierls treatment of the mode III elliptical crack assumes that there is a periodic relationship between shear stress and slip displacement along the slip plane

intersecting the crack tip (Peierls 1940, Rice 1992). Immediately prior to dislocation nucleation, there is a distribution of slip discontinuity along the slip plane that ultimately reaches a point of instability with increased applied stress and results in the nucleation of a dislocation at the crack tip. Using this framework, the critical energy release rates at the point of instability have been obtained for various values of crack length and crack tip root radius.

For most of our calculations, the simplest relationship between shear stress and slip displacement on the slip plane is assumed. In this section we exclusively use the Frenkel sinusoidal function

$$\tau = \frac{\mu b}{2\pi h} \sin\left(\frac{2\pi\Delta}{b}\right) = \frac{\pi\gamma_{us}}{b} \sin\left(\frac{2\pi\Delta}{b}\right), \quad (5)$$

where τ is the shear stress, Δ is the relative atomic displacement between two atomic planes, h is the interplanar spacing of those two planes and b is the burgers vector. As introduced by Rice (1992), the continuum analogue to Δ (referred to as δ) is thought of as Δ extrapolated to an imaginary cut half-way between the slipping planes and is given by

$$\delta = \Delta - \frac{\tau h}{\mu}. \quad (6)$$

We impose equilibrium along the slip plane using the integral equation:

$$\tau[\delta(r)] = \sigma_{\theta z}(r) - \frac{1}{b} \int_0^{\infty} \sigma_{\theta z}^{\text{self}}(r, s) \frac{\partial \delta}{\partial s} ds \quad (7)$$

where $\sigma_{\theta z}(r)$ is the pre-existing shear stress along the slip plane due to the applied load on the crack geometry (as used in equation (1)), and $\sigma_{\theta z}^{\text{self}}(r, s)$ is the stress at r along the cut due to a screw dislocation located at s , as provided by Zhang and Li (1991). Using the numerical procedure of Beltz (1992), the nonlinear integral equation is solved for incremental increases in the applied load until the instability is reached, coinciding with the emission of a dislocation.

Fixing the value of $\theta = 0^\circ$, figure 5 shows the critical energy release rates for various values of crack length and crack tip root radius. All quantities are normalized as in the previous section. The same calculations are performed for $\theta = 60^\circ$ and are shown in figure 6. The results from the Peierls framework produce the same trends as those performed under the Volterra framework, with striking agreement. As the crack tip root radius or crack length increases, so does the critical energy release rate.

As explained earlier, this model assumes a periodic relationship between the shear stress and the slip displacement along the slip plane. Figure 7 shows the slip displacement profile along the slip plane, $\theta = 60^\circ$, at the point of instability for a normalized crack length of 1000 and various values of the crack tip root radius. For sharper crack tip geometries, the slip displacement is relatively large in the immediate vicinity of the crack tip and dies off rapidly with increasing distance from the tip. In fact, the shear displacement at the sharp crack tip, just at instability, agrees very well with the value of $b/2$ predicted by the analysis of Rice (1992). For the blunter geometries, the slip displacement occurs over a much wider zone along the slip plane but maintains comparatively low levels of slip up to the point of instability.

Figure 8 shows the applied energy release rate versus the slip displacement at the crack tip for the same crack length and θ . As anticipated, these curves flatten, with zero slope, at the point of instability, indicating a local maximum in the 'applied'

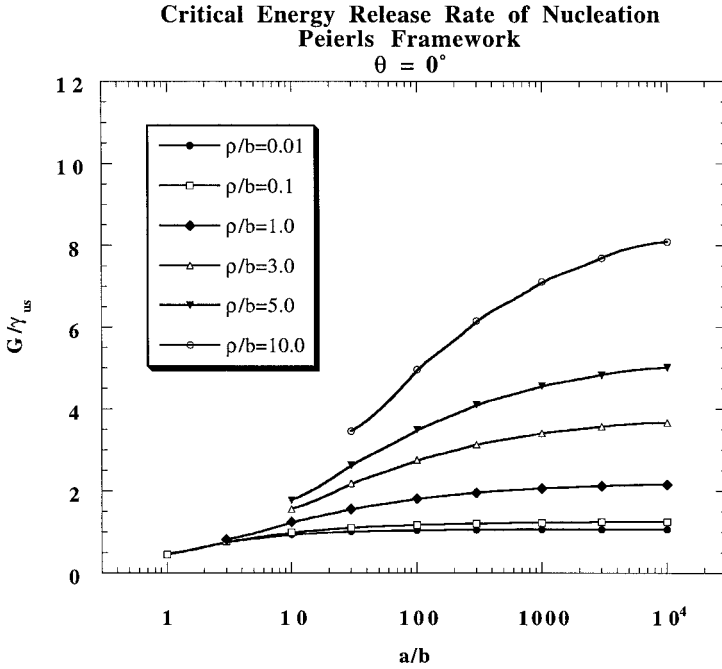


Figure 5. The critical energy release rates of screw dislocation nucleation for a slip plane inclination of 0° under mode III loading in the Peierls framework. Results are shown for various crack lengths and crack tip root radii.

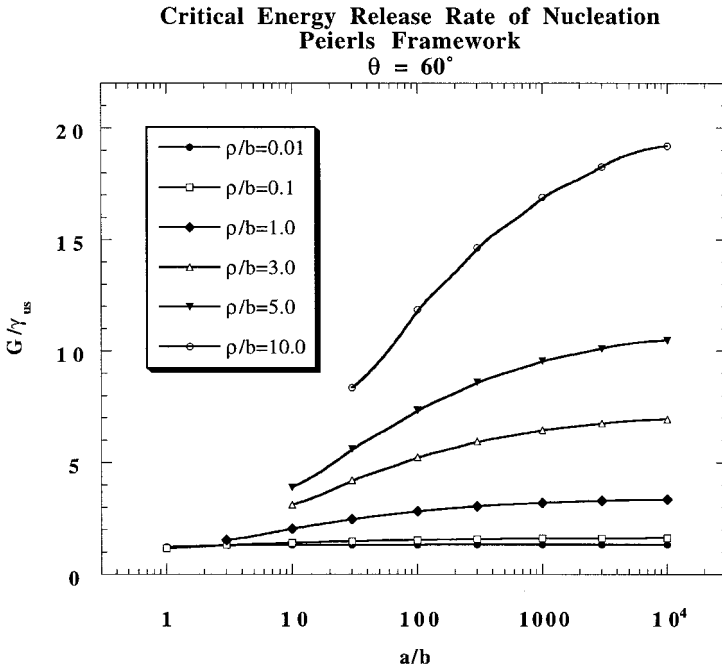


Figure 6. The critical energy release rates of screw dislocation nucleation for a slip plane inclination of 60° under mode III loading in the Peierls framework. Results are shown for various crack lengths and crack tip root radii.

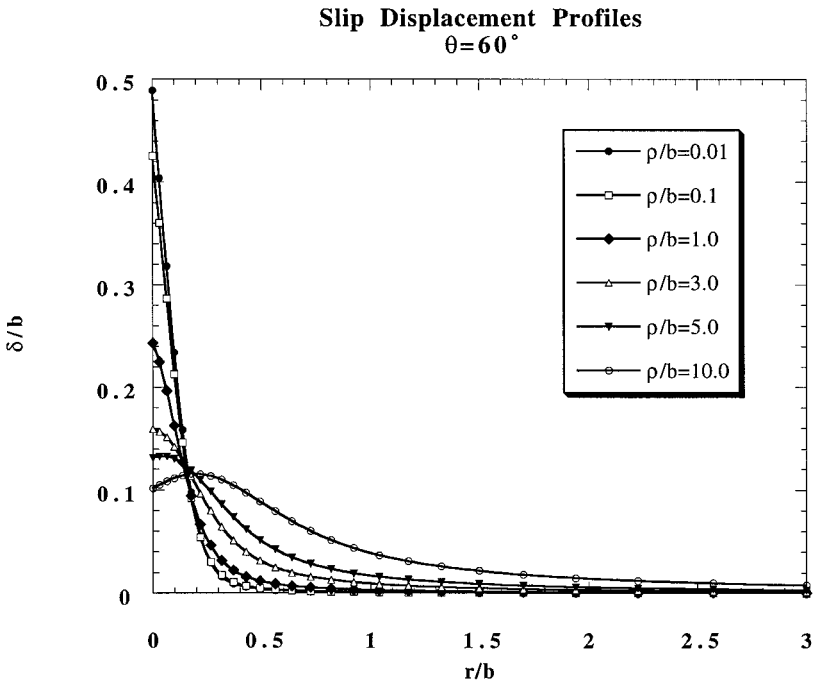


Figure 7. Slip displacement profiles along the 60° inclined slip plane for a normalized crack length of 1000 for various crack tip root radii under mode III loading at the point of dislocation nucleation.

energy release rate. As previously observed, increasing the bluntness of the crack tip increases the critical energy release rate for dislocation emission but lowers the slip discontinuity at which the instability occurs.

§4. EFFECT OF LEDGE CORRECTION AND UNSTABLE STACKING ENERGY

It has been pointed out by several authors that the Frenkel model, as used in the previous section (equation (5)), fixes the unstable stacking energy at the value $\gamma_{us} = \mu b^2 / 2\pi^2 h$. The unstable stacking energy actually tends to be smaller, especially for metals (Beltz and Freund 1994). Moreover, atomistic studies (Gumbsch and Beltz 1995, Xu *et al.* 1995) have suggested that the formation of a ‘ledge’, or additional atomic step, at a surface or crack tip retards dislocation formation. More realistic shear stress–displacement relationships have been formulated to account for these effects and can be used in the left-hand side of equation (7). We use the modified analytical form proposed by Xu *et al.* (1995):

$$\tau(\Delta) = \frac{\mu b}{2\pi^2 h} \left\{ \frac{\pi}{\beta} \sin\left(\frac{2\pi\Delta}{b}\right) + \frac{\pi(\beta-1)}{2\beta} \sin\left(\frac{4\pi\Delta}{b}\right) + \frac{\lambda \exp(-\lambda s/b)}{2q\beta} \left[1 - \cos\left(\frac{2\pi\Delta}{b}\right) \right] \right\}. \quad (8)$$

In equation (8), $\beta = \mu b^2 / 2\pi^2 h \gamma_{us}$ is an adjustable parameter that allows a variation in the unstable stacking energy from that consistent with the Frenkel model. In most cases, the value of β is greater than unity but less than two. The parameter q is

Applied Energy Release Rate versus Slip
 $\theta = 60^\circ$

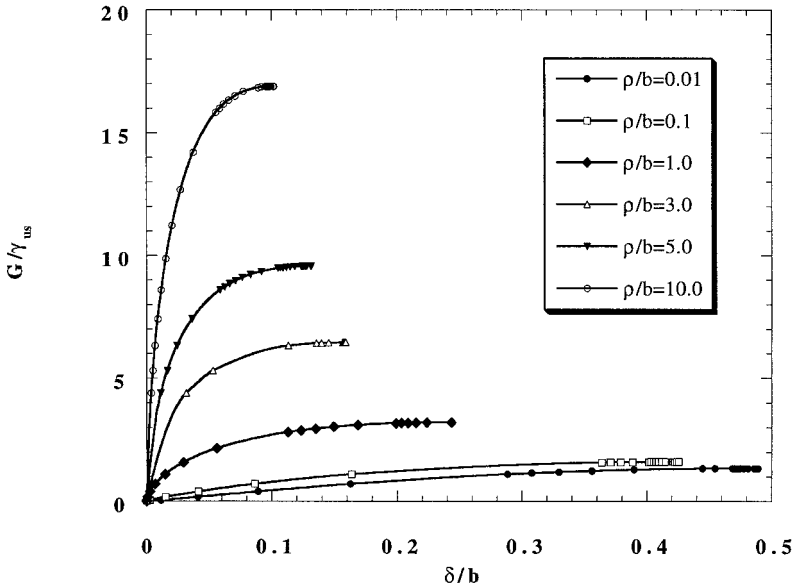


Figure 8. Applied energy release rates versus slip at the tips of mode III loaded elliptical cracks of normalized length equal to 1000 for various crack tip root radii.

defined as $\gamma_{us}/2\gamma_s$, where γ_s is the surface energy used to approximate the energy created during the ledge formation. Small values of q typify ductile materials while large values of q are associated with brittle materials (Sun *et al.* 1993). The value of q is generally less than unity. The parameter s is distance from the crack tip, and λ is a dimensionless parameter which characterizes the length scale over which the ledge or any surface perturbs the nominal τ versus Δ relationship. The value of λ is expected to lie between unity and two (Xu *et al.* 1995).

Figure 9 shows the critical energy release rates for cracks of normalized crack tip root radii equal to 3.0 with different crack lengths and various values of β and λ . For these calculations, $\theta = 60^\circ$ and $q = 0.125$. For the range of values examined, increasing the value of β decreases the critical energy release rate for dislocation nucleation. Conversely, considering the effect of ledge formation, an increase in the value of λ will subsequently increase the critical energy release rate for dislocation nucleation. Simultaneously considering greater values of unstable stacking energy and the effect of ledge formation will result in critical energy release rates that are greater than those found using the Frenkel model.

§5. SUMMARY

The two continuum frameworks used in this paper indicate that the critical threshold for dislocation formation is strongly dependent upon the crack length and crack tip geometry. The results show that increasing the crack tip root radius (i.e. the 'bluntness' of the crack) dramatically increases the required applied energy release rate to emit a dislocation from the crack tip. It is also shown that decreasing the crack length to below about 10^2 – 10^4 Burgers vectors causes the critical energy

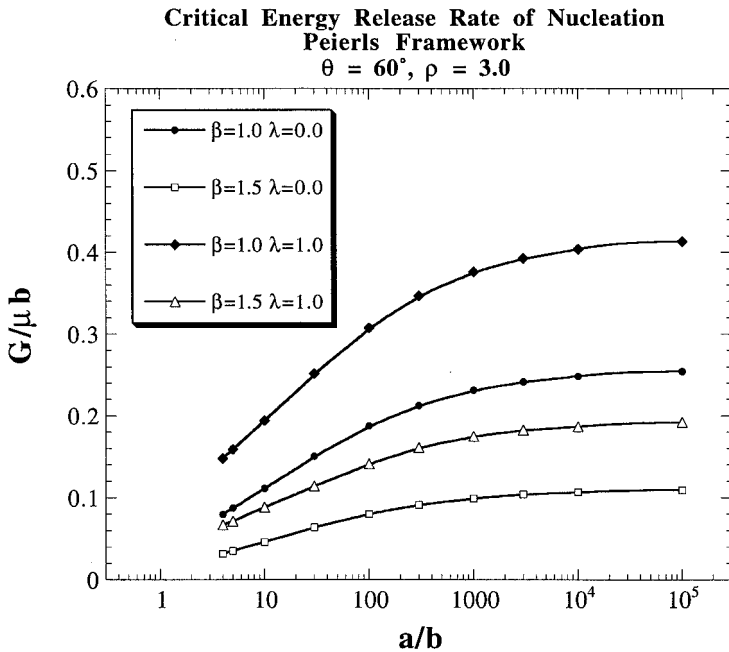


Figure 9. The critical energy release rates of screw dislocation nucleation for slip plane inclination of 60° and normalized crack tip root radius of 3.0 under mode III loading. Results are shown for various crack lengths, unstable stacking energies and ledge effect parameters.

release rate to fall substantially below the asymptotic value that corresponds to that of a semi-infinite crack. As noted in the introduction, the use of an idealized elliptical profile to represent a blunted crack tip should render these results, at best, over-estimates of the effects of blunting.

Furthermore, the magnitude of the critical energy release rate can be altered by considering the effects of ledge formation and realistic values of the unstable stacking energy. Smaller unstable stacking energies will reduce the critical energy release rate of dislocation nucleation, while ledge formation increases the critical energy release rate. These findings warrant a serious re-examination of continuum models that predict the outcome of the competition between dislocation nucleation and crack initiation. Perhaps more importantly, these effects should significantly contribute towards a reconciliation between continuum and atomistic models for dislocation nucleation as well as ductile versus brittle behaviour.

ACKNOWLEDGEMENTS

This research was supported by the National Science Foundation under awards CMS-9634647 and INT-9707863. Insightful discussions with Dr František Kroupa and Dr L. B. Freund are gratefully acknowledged.

REFERENCES

BELTZ, G. E., 1992, PhD Thesis, Division of Applied Sciences, Harvard University, Cambridge, Massachusetts.

- BELTZ, G. E., and FREUND, L. B., 1994, *Phil. Mag. A*, **69**, 183.
- FISCHER, L. L., and BELTZ, G. E., 1997, *Modelling Simul. Mater. Sci. Engng*, **5**, 517; 1998 (in preparation).
- FRENKEL, J., 1926, *Z. Phys.*, **37**, 572.
- GUMBSCH, P., 1995, *J. Mater. Res.*, **10**, 2897.
- GUMBSCH, P., and BELTZ, G. E., 1995, *Modelling Simul. Mater. Sci. Engng*, **3**, 597.
- MASON, D., 1979, *Phil. Mag.*, **39**, 455.
- PASKIN, A., MASSOUMZADEH, B., SHUKLA, K., SIERADZKI, K., and DIENES, G. J., 1985, *Acta metall.*, **33**, 1987.
- PEIERLS, R. E., 1940, *Proc. phys. Soc.*, **52**, 23.
- RICE, J. R., 1992, *J. Mech. Phys. Solids*, **40**, 239.
- RICE, J. R., BELTZ, G. E., and SUN, Y., 1992, *Topics in Fracture and Fatigue*, edited by A. S. Argon (New York: Springer), p. 1.
- RICE, J. R., SUO, Z., and WANG, J. S., 1990, *Metal-Ceramic Interfaces*, Vol. 4, edited by M. Rühle, A. G. Evans, M. F. Ashby and J. P. Hirth (Oxford: Pergamon), p. 269.
- RICE, J. R., and THOMSON, R., 1974, *Phil. Mag.*, **29**, 73.
- SCHIÖTZ, J., CANEL, L. M., and CARLSSON, A. E., 1997, *Phys. Rev. B*, **55**, 6211.
- SCHIÖTZ, J., CARLSSON, A. E., CANEL, L. M., and THOMSON, R., 1996, *Mater. Res. Soc. Symp. Proc.*, **409**, 95.
- SUN, Y., BELTZ, G. E., and RICE, J. R., 1993, *Mater. Sci. Engng*, **A170**, 67.
- XU, G., ARGON, A. S., and ORTIZ, M., 1995, *Phil. Mag. A*, **72**, 415.
- ZHANG, T., and LI, J. C. M., 1991, *Mater. Sci. Engng*, **A142**, 35.